

# Extinction bias of microlensed stars towards the LMC and the fraction of machos in the halo

HongSheng Zhao

Sterrewacht Leiden, Niels Bohrweg 2, 2333 CA, Leiden, The Netherlands  
 (hsz@strw.LeidenUniv.nl)

## ABSTRACT

We study the effect of reddening on microlensed stars towards the LMC. If lenses are in the LMC disk, then the source stars should be at the far side or behind the LMC disk. Thus they should experience more reddening and extinction by dust in the LMC disk than typical stars in the immediate neighbouring lines of sight. We simulate this effect in a variety of models for the LMC stars and dust. We stress that the optical depth is not one number, but a function of the reddening of the survey stars. We discuss how these effects could be used to constrain the fraction of machos in the dark halo. The effect of patchiness of dust can be controlled by working with faint stars in the smallest patches of the sky around the microlensed stars. This can be done most effectively with the Hubble Space Telescope in the ultra-violet. The non-detection of the reddening bias would be strongly in favor of machos in the Galactic halo.

*Subject headings:* dust, extinction — Magellanic Clouds — Galaxy: structure

## 1. Introduction

One of the main puzzles of Galactic microlensing surveys is the poorly determined location of the lens population of the events towards the Magellanic Clouds. Currently there are two popular views on the issue: (a) the lenses are located in the halo, hence are likely baryonic dark matter candidates (Alcock et al. 1997); (b) both the lenses and sources are part of the Magellanic Clouds, hence are stars orbiting in the potential well of the Clouds (Sahu 1994, Wu 1994, Zhao 1998a,b, 1999a, Weinberg 1999). These lead to drastically different predictions the relative amount of baryonic dark matter in galaxy halos as compared to baryons in stars and gas of various phases in galaxies and intergalactic medium. Gould (1995) showed that the low dispersion of many LMC tracers limits the amount of self-lensing in a virialized disk of the LMC, as assumed in original models of Sahu and Wu. Zhao (1998a) suggested that this constraint can be circumvented by invoking a plausible amount of unvirialized material, particularly tidally excited material in the immediate surrounding of the LMC disk, as either foreground lenses or background sources. Zhao (1998b) suggested that the polar stream seen in Kunkel et al.’s (1997) kinematic survey of the LMC carbon stars could contribute to lensing. Weinberg (1999) showed a specific model for

thickening the LMC disk by interaction with the Galaxy. Presently the observational status is still very confusing. Several observations suggest that our line of sight to the LMC passes through a 3-dimensional stellar distribution more extended in the line of sight than a simple thin disc of the LMC (Kunkel et al. 1997, Zaritsky et al. 1997, 1999 and references therein). Zaritsky et al. (1999) also include a review of the arguments and counter-arguments for these structures.

To break the degeneracy of the models we need new observations which are sensitive to the thickness of the LMC and the location of the lenses. Several ways have been proposed, including studying the spatial distribution and magnitude distribution of the microlensed sources (Zhao 1999a, Zhao, Graff & Guhathakurta 1999), the radial velocity distribution of the sources (Zhao 1999b) and the reddening distribution of the sources (Zhao 1999c). Essentially if lensing is due to Galactic halo machos or a foreground object, the sample of lensed stars should be a random subsample of the observed stars in the LMC. On the other hand, if there are some tidal material behind the LMC disk, then the stars in the tidal debris can be strongly lensed by ordinary stars in the intervening LMC disk, hence the spatial and kinematical distributions of these source stars will be those of the tidal debris, rather than those of the LMC disk. It is suggested that the source stars in the tidal debris should stand out as outliers in the radial velocity distribution of the LMC (Zhao 1999b), or fainter-than-normal red clump stars in the color magnitude diagram (Zhao, Graff & Guhathakurta 1999).

The idea about the reddening distribution is to measure the distribution of the reddening of individual LMC stars in small patches of sky centered on the microlensed stars. Basically some kind of “reddening parallaxes” can be derived for these stars from the line of sight depth effect, i.e., the dust layer in the LMC makes stars behind the layer systematically redder than those in front of the layer. The method involves obtaining multi-band photometry and/or spectroscopy of fairly faint (19 – 21mag) stars during or well after microlensing. From these data we can infer the reddening of microlensed stars and neighbouring unlensed stars. The method, in some sense, is a variation of the distance effect suggested by Stanek (1995) for the Galactic bulge microlensing events.

Here we extend the analysis of Zhao (1999c) and present simulations of the reddening of microlensed sources and show how reddening might be used to constrain the macho fraction in the halo. The models are described in §2, results are shown in §3. We summarize in §4 and discuss a few practical issues.

## 2. Models

## 2.1. Density models for the dust, the stars and the lenses

For the time being we shall assume a smoothed dust layer of the LMC with a  $\text{sech}^2$  profile and a FWHM of  $w$ . Let  $\rho_d(D)$  be the dust density at distance  $D$ , then

$$\rho_d(D)dD = \rho_d(D_{\text{LMC}})\text{sech}^2\left(\frac{D - D_{\text{LMC}}}{0.56w}\right)dD, \quad (1)$$

where  $\rho_d(D_{\text{LMC}})$  is the dust density at the mid-plane of the LMC.

For the LMC stars, we assume a two-component model. Let  $\rho_{\text{LMC}}(D)$  be the density of the LMC stars, then

$$\rho_{\text{LMC}}(D) = \frac{\Sigma_{\text{disk}}}{0.56W}\text{sech}^2\left(\frac{|D - D_{\text{LMC}}|}{0.56W}\right) + \frac{\Sigma_{\text{extra}}}{1.06W_{\text{extra}}}\exp\left[-0.69L^2\right], \quad (2)$$

where

$$L = \frac{(D_{\text{max}} - D_{\text{min}})(D - D_{\text{extra}})}{(D_{\text{max}} - D_{\text{extra}})W_{\text{extra}}}, \quad \text{if } D_{\text{max}} > D > D_{\text{extra}}, \quad (3)$$

$$= \frac{(D_{\text{max}} - D_{\text{min}})(D - D_{\text{extra}})}{(D_{\text{extra}} - D_{\text{min}})W_{\text{extra}}}, \quad \text{if } D_{\text{min}} < D < D_{\text{extra}}. \quad (4)$$

Our LMC model includes a (thin)  $\text{sech}^2$ -disk component of a surface density  $\Sigma_{\text{disk}}$  and FWHM thickness  $W$ , and an extra component with a surface density  $\Sigma_{\text{extra}}$  and FWHM thickness  $W_{\text{extra}}$ . The extra component consists of two half-Gaussians, which are joined together at their peaks at  $D = D_{\text{extra}}$  and truncated at the lower and upper ends at  $D = D_{\text{min}}$  and  $D = D_{\text{max}}$ . This is intended to model any non-virialized material in the vicinity of the LMC (Zhao 1998a, Weinberg 1999). To be most general, an offset between the extra component and the LMC disk, namely  $D_{\text{extra}} \neq D_{\text{LMC}}$ , is allowed in our models.

Let  $\nu_*(D)dD$  be the number of LMC star in a line of sight distance bin  $(D, D + dD)$ , then the LMC star number density will be given by

$$\nu_*(D)dD = C_0\rho_{\text{LMC}}(D)D^2dD, \quad (5)$$

where  $C_0$  is a normalization constant.

For the lens population, we include the contribution from the LMC stars and intervening machos in an isothermal halo. The density of lenses at distance  $D_l$  is

$$\rho_{\text{lens}}(D_l) = \rho_{\text{LMC}}(D_l) + f_{\text{macho}}\rho_{\text{halo}}(D_l), \quad (6)$$

where  $f_{\text{macho}}$  is the fraction of machos in the halo, and  $\rho_{\text{halo}}(D)$  is the dark halo density given by

$$\rho_{\text{halo}}(D) = 0.01M_{\odot}\text{pc}^{-3}\left[1 + \left(\frac{D}{8\text{kpc}}\right)^2\right]^{-1}. \quad (7)$$

The halo density corresponds to a surface density of dark matter (machos plus wimps) halo  $\Sigma_{\text{halo}} \sim 100M_{\odot}\text{pc}^{-2}$  towards the LMC.

## 2.2. Reddening vs. line of sight distance of a star and their distributions

In general the reddening of a star is correlated with the distance to the star, with stars at the backside of the LMC seeing more dust and experiencing more reddening. But since the dust distribution is clumpy and the reddening distribution is patchy, any relation between the reddening and the line of sight distance is not a well-defined one-to-one relation, but has a significant amount of scatter due to patchiness of dust and measurement error. Nevertheless we can argue that stars in a small (e.g.,  $4'' \times 4''$ ) patch of sky will see the same set of dust clouds, so if we sort these neighbouring stars according their reddening, we also get a sorted list in distance.

Stars in the LMC can be ranked according to an observable reddening indicator  $\kappa_{\text{obs}}$ . For any LMC star define

$$\kappa_{\text{obs}} \equiv \frac{E(B - V)_{\text{LMC}}^{\text{obs}}}{\langle E(B - V)_{\text{LMC}}^{\text{obs}} \rangle}, \quad (8)$$

where  $E(B - V)_{\text{LMC}}^{\text{obs}}$  is the observed reddening in  $B - V$  color towards the LMC star, after discounting the reddening by the Galactic foreground, and  $\langle E(B - V)_{\text{LMC}}^{\text{obs}} \rangle$  is the average over random stars in the small patch of sky centered on that LMC star, and is approximately the reddening of those stars at the mid-plane of the LMC. Surely the typical reddening  $\langle E(B - V)_{\text{LMC}}^{\text{obs}} \rangle$  varies widely from patches to patches on scales of arcmins (Harris et al. 1997 and references therein), but the rescaled reddening  $\kappa_{\text{obs}}$  allows us to sort the stars not only in the same patch but also stars in different patches. A higher rank, i.e. a larger  $\kappa_{\text{obs}}$ , means a deeper penetration into the dust layer. Stars at the midplane have a rank  $\kappa_{\text{obs}} = 1$ , and those at the front or back side of the LMC disk have a rank  $\kappa_{\text{obs}} = 0$  or  $\kappa_{\text{obs}} = 2$ .

Consider the reddening rank of stars in a smooth dust model. Let  $A_{\text{LMC}}(D)$  be the dust absorption towards a LMC star at distance  $D$  (after discounting the absorption by the Galactic foreground dust), and let  $\kappa(D)$  be the predicted reddening rank of the star, then

$$\kappa(D) = \frac{A_{\text{LMC}}(D)}{A_{\text{LMC}}(D_{\text{LMC}})} = \frac{\int_0^D \rho_d(D) dD}{\int_0^{D_{\text{LMC}}} \rho_d(D) dD} \quad (9)$$

(cf eq. 1), where  $\rho_d(D_{\text{LMC}})$  and  $A_{\text{LMC}}(D_{\text{LMC}})$  are the dust density and absorption at the mid-plane of the LMC. It is easy to show that

$$\kappa(D) = 1 + \tanh\left(\frac{D - D_{\text{LMC}}}{0.56w}\right) \quad (10)$$

$$= 0, \quad D - D_{\text{LMC}} \ll w \quad (11)$$

$$= 1, \quad D = D_{\text{LMC}} \quad (12)$$

$$= 2, \quad D - D_{\text{LMC}} \gg w. \quad (13)$$

So the reddening rank  $\kappa(D)$  increases from 0 to 2 abruptly in the distance range  $D_{\text{LMC}} \pm \frac{w}{2}$  as a star enters and exits the dust layer. It turns out that this property is not limited to  $\text{sech}^2$  profile dust, but generic for smooth dust layer of a symmetric profile.

Now to take into account of the scatter due to measurement error and any residual patchiness, we assume that the observed reddening has a simple Gaussian distribution centered on the predicted value from a smooth dust disk model. Then for a star at any distance  $D$ , the reddening rank  $\kappa_{\text{obs}}$  is drawn from the following distribution function

$$B(\kappa_{\text{obs}}, D) = \frac{1}{\sqrt{2\pi}\sigma} \exp \left[ -\frac{(\kappa_{\text{obs}} - \kappa(D))^2}{2\sigma^2} \right], \quad (14)$$

which is a Gaussian with a constant dispersion  $\sigma$ , and a mean  $\kappa(D)$  as predicted from a smooth model.

Now we integrate over LMC stars at all distance and bin them according to their reddening  $\kappa_{\text{obs}}$ . Let  $N_*(\kappa_{\text{obs}})$  be the relative frequencies of finding an unlensed star with a reddening  $\kappa_{\text{obs}}$ , then

$$N_*(\kappa_{\text{obs}}) = \int dD \nu_*(D) B(\kappa_{\text{obs}}, D). \quad (15)$$

### 2.3. Optical depth as a function of distance and reddening

The microlensing optical depth  $\tau(D_s)$  of a source star at distance  $D_s$  is defined by

$$\tau(D_s) \equiv \frac{\nu_s(D_s)}{\nu_*(D_s)} \quad (16)$$

where  $\nu_*(D_s)dD_s$  and  $\nu_s(D_s)dD_s$  are the numbers of stars and microlensed sources in the distance bin  $(D_s, D_s + dD_s)$  respectively (cf. eq. 5). It is well-known that in the standard full-macho isothermal halo model  $f_{\text{macho}} = 1$ ,  $\rho_{\text{lens}} = \rho_{\text{halo}}$  (cf. eq. 6), and the microlensing optical depth  $\tau_{\text{std}} = 5 \times 10^{-7}$  (cf. e.g., Paczyński 1986). It is convenient to rescale the optical depth of a model with this standard value. The microlensing optical depth  $\tau(D_s)$  is then given by

$$\tau(D_s) = \tau_{\text{std}} \frac{\int_0^{D_s} dD_l \rho_{\text{lens}}(D_l) (D_s - D_l) D_l / D_s}{\int_0^{D_{\text{LMC}}} dD_l \rho_{\text{halo}}(D_l) (D_{\text{LMC}} - D_l) D_l / D_{\text{LMC}}}. \quad (17)$$

The optical depth  $\tau(D_s)$  increases with the source distance. Suppose all lenses are at distance  $D_l$ , then

$$\tau(D_s) \sim (D_s - D_l). \quad (18)$$

Unfortunately, it is difficult to observe this effect because it is hard to measure the distance to a LMC star at the accuracy of 1 kpc. But fortunately the distance to a star is correlated with the reddening, and the reddening of a star can be measured accurately to 20%. So we have an interesting effect that the rate of microlensing is correlated with the reddening of the stars. For each bin in terms of the rank of reddening  $(\kappa_{\text{obs}}, \kappa_{\text{obs}} + d\kappa_{\text{obs}})$ , we can define an optical depth

$$\tau_{\text{obs}}(\kappa_{\text{obs}}) \equiv \frac{N_s(\kappa_{\text{obs}})}{N_*(\kappa_{\text{obs}})} = \frac{\int dD_s \nu_s(D_s) B(\kappa_{\text{obs}}, D_s)}{\int dD \nu_*(D) B(\kappa_{\text{obs}}, D)}, \quad (19)$$

where  $N_*(\kappa_{\text{obs}})$  and  $N_s(\kappa_{\text{obs}})$  are the relative frequencies of finding an unlensed star and a microlensed source with reddening  $\kappa_{\text{obs}}$  respectively (cf. eq. 15).

Note  $\tau_{\text{obs}}(\kappa_{\text{obs}})$  is a function measurable observationally because we can always bin the microlensed events according their observable reddening, and get their frequencies  $N_*(\kappa_{\text{obs}})$  and  $N_s(\kappa_{\text{obs}})$ . Of particular interest is  $\tau_{\text{obs}}(0 < \kappa_{\text{obs}} \leq 1)$ . Note stars at the mid-plane of the LMC disk have average reddening, so  $\kappa_{\text{obs}} \sim 1 \pm 3\sigma$  at  $3\sigma$  confidence level. In comparison stars well in front of the dust layer have  $\kappa_{\text{obs}} < 3\sigma$ , and stars well behind the dust layer have  $\kappa_{\text{obs}} > 2 - 3\sigma$ . So  $\tau_{\text{obs}}(0 < \kappa_{\text{obs}} \leq 1)$  is the optical depth of a thin layer of stars co-spatial with the dust layer and slightly closer to us the mid-plane of the LMC with  $D_{\text{LMC}} - w/2 \leq D \leq D_{\text{LMC}}$ . Since the thickness of the dust layer  $w \sim 100 - 200\text{pc}$  is very small, these stars are virtually at the same distance. So we have

$$\tau_{\text{obs}}(0 < \kappa_{\text{obs}} \leq 1) \approx \tau(D_{\text{LMC}}) \geq f_{\text{macho}}\tau_{\text{std}}. \quad (20)$$

So we have turned the theoretical quantity  $\tau(D_{\text{LMC}})$  to an observable, and this observable optical depth  $\tau_{\text{obs}}(0 < \kappa_{\text{obs}} \leq 1)$  sets an upper limit on the amount of machos in the foreground of the LMC. The above inequality reduces an equality in the absence of any LMC lenses in front of the LMC disk.

If the picture that the LMC is a thin disk without any extra material in the front or back is correct, then we should find that  $\tau_{\text{obs}}(\kappa_{\text{obs}})$  is at a constant level  $\approx \tau(D_{\text{LMC}}) = f_{\text{macho}}\tau_{\text{std}}$  for all reddening.

Presently the survey teams have not studied the reddening dependence of the optical depth, so they quote only the observed optical depth averaged over all LMC stars, which is only one number. Let this be  $\langle \tau_{\text{obs}} \rangle$ , then current data require

$$\langle \tau_{\text{obs}} \rangle \equiv \frac{\int_{D_{\text{min}}}^{D_{\text{max}}} dD \nu_*(D) \tau(D)}{\int_{D_{\text{min}}}^{D_{\text{max}}} dD \nu_*(D)} = \frac{\int d\kappa_{\text{obs}} N_*(\kappa_{\text{obs}}) \tau(\kappa_{\text{obs}})}{\int d\kappa_{\text{obs}} N_*(\kappa_{\text{obs}})} \approx 0.5\tau_{\text{std}}, \quad (21)$$

where the factor 0.5 comes from the fact that the observed microlensing optical depth account for about one-half of that of the standard macho dark halo model  $\tau_{\text{std}}$  (Alcock et al. 1997).

We would like to know how much of the observed optical depth is due to stellar lenses in the LMC vicinity and how much is due to machos in Galactic halo. If we define  $f_*$  as the fraction of the observed microlensing depth due to stellar lenses, then the fraction of machos in the dark halo is given by

$$f_{\text{macho}} = \frac{\langle \tau_{\text{obs}} \rangle (1 - f_*)}{\tau_{\text{std}}} = 0.5(1 - f_*). \quad (22)$$

So for a given set of stellar distribution parameters  $\Sigma_{\text{extra}}$  etc, we can predict the optical depth due to stellar lenses  $f_*\tau_{\text{std}}$ , we can then determine  $f_{\text{macho}}$  by fixing the overall optical depth to the observed value.

Finally we would like to characterize the excess reddening of the microlensed stars. This can

be done by defining an observable parameter  $\xi_{\text{obs}}$  such that

$$\xi_{\text{obs}} \equiv \frac{\int d\kappa_{\text{obs}} N_s(\kappa_{\text{obs}}) \kappa_{\text{obs}}}{\int d\kappa_{\text{obs}} N_s(\kappa_{\text{obs}})} - \frac{\int d\kappa_{\text{obs}} N_*(\kappa_{\text{obs}}) \kappa_{\text{obs}}}{\int d\kappa_{\text{obs}} N_*(\kappa_{\text{obs}})} \quad (23)$$

$$= \frac{\int dD \nu_s(D) \kappa(D)}{\int dD \nu_s(D)} - \frac{\int dD \nu_*(D) \kappa(D)}{\int dD \nu_*(D)}. \quad (24)$$

Because of the integration over the entire range of the reddening,  $\xi_{\text{obs}}$  is independent of the dispersion  $\sigma$  between the observed reddening rank of a star and the reddening rank predicted from a smooth model (cf. eq. 14).

### 3. Results

#### 3.1. Model parameters

Here we study the effect of a mixed halo model on the reddening distribution of the microlensed stars. Since the parameters of the LMC are very uncertain, we will explore a range of dust models and stellar models. Table 1 lists the parameters for the models.

We fix the distance to the LMC  $D_{\text{LMC}} = 50\text{kpc}$ , and set the tidal radius of the LMC  $|D_{\text{min}} - D_{\text{LMC}}| = |D_{\text{max}} - D_{\text{LMC}}| = 10\text{kpc}$ . For the  $\text{sech}^2$  stellar disk of the LMC and the dust layer, we fix  $\Sigma_{\text{disk}} = 400M_{\odot} \text{ pc}^{-2}$ . We fix the FWHM thickness of the dust layer  $w = 200 \text{ pc}$ , but allow the relative thickness of the two disks  $W/w$  to vary in the range 0.5 to 2, a reasonable range for thin stellar and dust disks. We set the FWHM of the tidal material  $W_{\text{extra}} = 0.05(D_{\text{max}} - D_{\text{min}}) = 1\text{kpc}$ , but allow the peak position to vary in the range  $40 \text{ kpc} \leq D_{\text{extra}} \leq 60 \text{ kpc}$ , and the amount of stars in extra component to vary in the range  $0 \leq \Sigma_{\text{extra}} \leq 50M_{\odot} \text{ pc}^{-2}$ . We set this upper limit for the surface density of the extra material to about 10% of the surface density of the LMC, an acceptable amount for some hidden material. In comparison the surface density of dark matter (machos plus wimps) halo  $\Sigma_{\text{halo}} \sim 100M_{\odot} \text{ pc}^{-2}$  (cf. eq. 7). These parameters are comparable to those of previous models for the volume density of the LMC disk (Wu 1995, Weinberg 1999).

It turns out the reddening distributions of microlensed and unlensed stars are insensitive to exact values of  $w$ ,  $W$ ,  $W_{\text{extra}}$  and  $\Sigma_{\text{disk}}$  as long as we are in the regime where  $w \sim W \ll W_{\text{extra}} \ll |D_{\text{max}} - D_{\text{min}}|$  and  $\Sigma_{\text{extra}} \sim \Sigma_{\text{halo}} \ll \Sigma_{\text{disk}}$ . These distributions are more sensitive to the ratios such as  $W/w$ ,  $\Sigma_{\text{extra}}/\Sigma_{\text{halo}}$ , and  $\frac{|D_{\text{extra}} - D_{\text{LMC}}|}{|D_{\text{max}} - D_{\text{min}}|}$ . For example, models with the extra stars centered on the LMC disk, i.e.,  $\frac{|D_{\text{extra}} - D_{\text{LMC}}|}{|D_{\text{max}} - D_{\text{min}}|} \sim 0$ , require much more stars with  $\Sigma_{\text{extra}}/\Sigma_{\text{halo}} \gg 1$  for come up with enough events, hence are much less efficient than models with extra stars 5 – 10kpc in front or behind the LMC in terms of producing microlensing. So the main parameters that we will vary are  $\Sigma_{\text{extra}}$ ,  $D_{\text{extra}}$  and  $W/w$ . The predictions are made for halo-lensing models and mixed models with different amount of stars in the extra component and different offset distance from the LMC and the relative thickness of the stellar disk vs. the dust

disk.

We also set the random error  $\sigma$  for the observed reddening at 20%-40% level, which seems a reasonable amount. A larger dispersion would smooth out some tell-tale features of the reddening distributions. But it turns out that the mean excess  $\xi_{\text{obs}}$  and the optical depth in the mid-plane  $\tau_{\text{obs}}(\kappa_{\text{obs}} = 1)$  are insensitive to the observational error  $\sigma$ .

### 3.2. Reddening distributions of microlensed and unlensed stars

The line of sight distributions of a few model quantities are shown in Fig. 1 for one of the models (see caption). Clearly all stellar density distributions peak at  $D = D_{\text{LMC}} = 50\text{kpc}$ , the mid-plane of the high density disk of the LMC; similarly for the thin dust layer. The LMC stars have a second peak due to extra stars placed behind the LMC disk. The lens density distribution also has a gentle falling part in the range  $10 \text{ kpc} < D < 40 \text{ kpc}$  due to foreground machos, whose number density falls as  $D^{-2}$ . The lensed stars (dotted line with diamonds) also have a higher tail.

For sources in front the LMC disk  $D < D_{\text{LMC}}$  the microlensing optical depth is nearly constant,  $\tau(D_s)/\tau_{\text{std}} \sim f_{\text{macho}} \sim 0.36$ . This is because the optical depth due to the ever decreasing density of the foreground machos is insensitive to the source distance. But after passing the LMC disk the optical depth takes off linearly with the source distance till  $\tau(D_s)/\tau_{\text{std}} \gg 1$ . This is because any source star behind the LMC suddenly sees an intervening dense screen of lenses coming from the high surface density stellar disk of the LMC, so the optical depth goes up in proportional to the distance to the LMC disk (cf. eq. 18). This explains the higher tail of the lensed stars as compared to unlensed stars (cf. Fig. 1). Note that there is only a modest increase of the optical depth from entering to exiting the LMC thin disk. The amount is on the order of  $(\Sigma_{\text{disk}}/\Sigma_{\text{halo}})(W/10\text{kpc}) < 8\%$  of the total optical depth, consistent with the estimation of Sahu (1994) and Wu (1994) for a thin disk.

The dust extinction is nearly a Heaviside function of the distance, climbing steeply from zero absorption in front of the layer to a constant value  $2 \times A_{\text{LMC}}(D_{\text{LMC}})$  a few hundred pc behind the layer, where  $A_{\text{LMC}}(D_{\text{LMC}})$  is the absorption in the mid-plane. This is because as a star sinks deeper in the dust layer it experiences an increasing reddening before it emerges from the dust layer again.

Fig. 2 shows the reddening distributions of microlensed and unlensed stars. The distribution for unlensed stars (upper panels) hardly depends on parameters of the extra component  $\Sigma_{\text{extra}}$  and  $D_{\text{extra}}$ . It is only sensitive to the relative thickness of the stellar disk and the dust layer. At one end of the extreme, we have a thin dust layer and a thicker stellar disk ( $W/w = 2$ , solid lines). We see the familiar double-horn structure. This is because most stars in a thick disk are either in front of the dust layer and free from reddening or behind the layer and reddened by the maximum amount. At the opposite extreme, if the stellar disk is thinner than the dust layer ( $W/w = 0.5$ , dash-dot-dot lines), the distribution becomes peaky in the middle because

most stars of the thin disk are in the mid-plane of the dust layer, hence reddened by half of the maximum (back-to-front) value. In between if the dust layer and the stellar disk have the same scale height and are evenly mixed ( $W/w = 1$ , dashed lines), we have a flat top-hat distribution.

The distributions for the microlensed stars depend on the location and the amount of the extra component. For halo-lensing models, the distribution of lensed stars and unlensed stars are virtually indistinguishable (cf. Fig. 2a). The situation is largely unchanged if we move all lenses from the halo to 10 kpc in front of the LMC disk (cf. Fig. 2b). The extra component shows up merely as a marginal excess of low reddening stars in the unlensed stars, a small effect which might escape detection.

The situation is drastically different if we put even a small amount ( $\Sigma_{\text{extra}} = 10M_{\odot} \text{ pc}^{-2}$ , or 2.5%) of stars behind the LMC disk (Fig. 2c). The distribution are strongly skewed towards high reddening. This is because lensing favors source stars well-behind the lenses. More specifically if the lenses are machos midway to the LMC, or stars some 10 kpc in front of the LMC, then the probability of drawing a source star at 100 pc behind the dust layer is about 0.8% or 2% higher than drawing one at 100 pc in front of the dust layer (cf. eq. 18). So in average, the lensed sources should be more reddened than the unlensed ones by merely a few percent. In contrast, if the lenses are at mid-plane of the LMC, then nearly all sources will be behind the dust layer, and hence the reddening rank  $\kappa_{\text{obs}}$  increases by one (cf. eq. 8 and eq. 10).

In Fig. 2c there are still some source stars at low reddening because we allow for machos in the foreground. The skewness effect becomes stronger as we decrease the macho fraction, and increase the extra stars behind the LMC. For  $\Sigma_{\text{extra}} = 40M_{\odot} \text{ pc}^{-2}$  and  $D_{\text{extra}} = 60\text{kpc}$ , then all lensed sources should have an observed reddening rank  $\kappa_{\text{obs}} \approx 2$ . In this case  $f_{\text{macho}} \approx 0$  and all lenses come from the LMC disk.

Another way to quantify the above effects is to look at the observed optical depth as a function of the reddening rank of stars (cf. Fig. 3a). The plateau of the  $\tau_{\text{obs}}(\kappa_{\text{obs}})$  curves in the range  $0 < \kappa_{\text{obs}} \leq 1$  are for stars imbeded in the dust layer of the LMC. They are slightly closer to us than the stars at the mid-plane, for which  $\kappa_{\text{obs}} = 1 \pm 3\sigma$ , but are virtually at the same distances  $D_{\text{LMC}} \pm w/2$ . The plateau also set an upper limit on the optical depth of machos (cf. eq. 20).

On the other hand those stars with  $\kappa_{\text{obs}} \geq 2$  include both stars well behind the LMC disk, which have a very high optical depth (cf. the curve of  $\tau(D)$  in Fig. 1), and any Gaussian tail of the LMC disk stars due to random error of the reddening. So  $\tau_{\text{obs}}(\kappa_{\text{obs}})$  can have a high tail if the extra component behind the LMC is stronger than the Gaussian tail due to a non-zero dispersion  $\sigma$ . These results depend somewhat on the reddening and the relative thickness of the stellar disk and the dust layer (cf. Fig. 3b). A larger measurement error smoothes the sharp transition from the plateau to the high tail. The tail is lower if the stellar disk is thicker than the dust layer, because of more overlap in the observed reddening of the stars in the LMC disk and those well-behind the LMC.

Fig. 4 shows that in general a strong excess in reddening is seen in models with most of the

lenses in the LMC disk, and the sources behind the midplane of the LMC disk. Models with a high macho fraction  $f_{\text{macho}} \geq 0.4$  and/or with lenses being extra stars a few kpc well in front of the LMC disk predict only a modest amount of excess  $\xi_{\text{obs}} \leq 0.1$ . So these models could be ruled out if we measure a strong excess. In particular, if  $\xi_{\text{obs}} \geq 0.5$  then the dark halo cannot have more than 15% in machos. On the other hand, if the excess is small, then the interpretation remains non-unique. These results depends only slightly on the thickness of the dust layer with the thinner dust layer predicting a stronger excess. Given accurate reddening, it is possible to measure or at least set an upper limit on the fraction of dark matter in machos.

### 3.3. Empirical relations

We have also find a few empirical relations for converting the reddening excess  $\xi_{\text{obs}}$  to the macho fraction  $f_{\text{macho}}$ . Assuming that there are few stellar lenses in the immediate foreground of the LMC disk, which would be the case if  $0.8 \geq \xi_{\text{obs}} \geq 0.2$ , then to a good approximation, the fraction  $f_*$  of microlensing due to LMC stars is given by

$$f_* \approx 1.2\xi_{\text{obs}}. \quad (25)$$

The fraction of machos is related to  $\xi_{\text{obs}}$  by

$$f_{\text{macho}} \approx 0.5(1 - 1.2\xi_{\text{obs}}) \quad (26)$$

(cf. eq. 22 and 21). Here we have adopted the present reported value for the microlensing optical depth to the LMC, i.e., about half of that of the standard halo. But the results can be rescaled proportionally as more data become available.

The result can also be recast as following,

$$f_{\text{macho}} \approx \frac{\tau_{\text{obs}}(0 < \kappa_{\text{obs}} \leq 1)}{5 \times 10^{-7}} \quad (27)$$

(cf. eq. 20), where  $\tau_{\text{obs}}(0 < \kappa_{\text{obs}} \leq 1)$  is the optical depth of the LMC stars observed with lower than average reddening; these are stars sandwiched in a thin layer between the mid-plane of the LMC disk and the near side of the dust layer. The optical depth of the least reddened stars best approximates the optical depth of foreground machos, because it is least contaminated by stellar lenses in the LMC.

These relations work best if we can neglect stellar lenses in the immediate foreground of the LMC disk. But interestingly, these results are insensitive to the assumption of the dust distribution and stellar distribution of the LMC, e.g., the distance of the extra background material, and their surface density, the relative thickness of the dust layer and the stellar disk. We also allow for a realistic amount of measurement error and patchiness of extinction.

#### 4. Summary

In summary, we have studied effects of dust layer in the LMC on the microlensing events in a wide range of models of star and dust distributions in the LMC. We propose to bin LMC stars according to their reddening rank  $\kappa_{\text{obs}}$  (as defined in eq. 8), and study the observable microlensing optical depth as a function of the reddening rank  $\kappa_{\text{obs}}$ . We find that self-lensing models of the LMC draw preferentially sources behind the dust layer of the LMC, and hence can be distinguished from the macho-lensing models once the reddening by dust is measured.

If a low excess in reddening ( $\xi_{\text{obs}} < 0.2$ ) is observed then the interpretation would not be unique: the reddening distribution does not distinguish very well lensing by machos and lensing by stars a few kpc in front of the LMC. The optical depth can be explained equally well by a screen of macho lenses with  $\Sigma_{\text{extra}} = 50M_{\odot} \text{ pc}^{-2}$  at 10 kpc from the Sun, or by a screen of stellar lenses with a same surface density at 10 kpc in front of the LMC disk. As far as the reddening distributions are concerned, these two models are barely distinguishable (cf. Fig. 2ab). On the other hand the reddening distribution is very sensitive to any stars behind the LMC disk. If 2-3% of the LMC stars is put in an extra component 5 – 10 kpc behind the LMC, then we can see markedly different distribution in the microlensed stars (cf. Fig. 2c); this corresponds to a surface density  $\Sigma_{\text{extra}} = 10M_{\odot} \text{ pc}^{-2}$ . The signal gets even stronger as we decrease the macho fraction and increase the surface density of the background stars.

Our main finding is that among stars of different reddening rank, the optical depth of the least reddened stars  $\tau_{\text{obs}}(\kappa_{\text{obs}} \sim 0)$  is the closest approximation to the optical depth of machos (cf. Fig. 3). The macho fraction  $f_{\text{macho}}$  also correlates tightly with the excess reddening  $\xi_{\text{obs}}$  of the microlensed sources (cf. Fig. 4). These results are summarized by the empirical relations in the previous section. An observable high excess in reddening ( $1 > \xi_{\text{obs}} > 0.2$ ) would be a definitive signal for many LMC disk lenses and low macho fraction. Potentially we can constrain the fraction of Galactic dark matter in machos this way.

There are a number of problems to apply the method to observations. (a) Reddening of individual stars is difficult to measure accurately. Reddening can be determined by constructing reddening-free indices with photometry of three or more broad bands, or with low resolution spectroscopy. Typical accuracy is about 0.02 mag. in  $E(B - V)$  with these methods (Harris et al. 1997), which is about 20% of the typical reddening in the LMC (Harris et al. 1997). (b) Stars in the LMC are likely crowded from the ground. Blended images of stars lead to unphysical colors and spurious reddening. (c) Dust distribution is very clumpy. Extinction towards OB stars in the LMC disk can easily vary at a factor of two level among different patches of the sky separated by  $1'$  (Harris et al. 1997). (d) The effect of extinction by the dust layer of the Galaxy near the Sun should be included. Oestriecher et al. (1996) show that the Galactic foreground extinction is not entirely smooth. There are dark patches on  $30'$  scales.

The clumpiness of the dust, together with the fairly large error of the reddening vector measurable from broad-band photometry, can lead to a large scatter in the relation between

reddening and line of sight depth. Zhao (1999c) argue that these problems, particularly patchiness can be overcome if we restrict to the smallest patches of sky around each microlensing source where the variation is likely at only 20% level. Spectroscopic observation with the Hubble Space Telescope in the ultra-violet can in principle resolve many faint stars in the small patches around each microlensed stars, and measure the reddening accurately. By obtaining the reddening of stars in the present 20 – 30 microlensing lines of sight we should be able to measure the excess reddening confidently. We should also be able to bin the events in the reddening rank, and study the optical depth as a function of reddening. A null result of any variation of the optical depth would be in favor of a significant baryonic dark component of the Galaxy.

## REFERENCES

Alcock C. et al. 1997, ApJ, 486, 697 (astro-ph/9606165)

Gould, A. 1995, ApJ, 441, 77

Harris, J., Zaritsky, D. & Thompson, I., 1997, AJ, 114, 1933

Kunkel W., Demers S., Irwin M., & Albert L. 1997, ApJ, 488, L129

Oestreicher, M. O. & Schmidt-Kaler, T 1996, A&AS, 117, 303

Paczyński, B. 1986, ApJ, 304, L1

Sahu A. 1994, Nature, 370, 275

Stanek, K.Z. 1995, ApJ, 441, L29

Stanek, K.Z. 1996, ApJ, 460, L37

Weinberg M. 1999, astro-ph/9811204

Wu X.P. 1994, ApJ, 435, 66

Zaritsky, D. & Lin, D. 1997, AJ, 114, 2545

Zaritsky D., Shectman S.A., Thompson I.; Harris J., Lin D.N.C. 1999, AJ, 117, 2268

Zhao, H.S. 1998a, MNRAS, 294, 139

Zhao, H.S. 1998b, ApJ, 500, L49

Zhao, H.S. 1999a, Particle Physics and the Early Universe, AIP Proc. ed. David Caldwell (astro-ph/9902179)

Zhao, H.S. 1999b, ApJ, 526, 000 (astro-ph/9906126)

Zhao, H.S. 1999c, ApJ, 527, 000 (astro-ph/9906214)

Table 1. Fixed parameters for the stellar, dust and halo models

$\Sigma_{\text{disk}}$	$W_{\text{extra}}$	$D_{\text{min}}$	$D_{\text{max}}$	$w$	$\langle \tau_{\text{obs}} \rangle$	$\tau_{\text{std}}$	$\Sigma_{\text{halo}}$
$400M_{\odot}\text{pc}^{-2}$	1kpc	40kpc	60kpc	200pc	$2.9 \times 10^{-7}$	$4.7 \times 10^{-7}$	$200M_{\odot}\text{pc}^{-2}$

Zhao, H.S., Graff, D. & Guhathakurta, P. 1999, ApJ submitted (astro-ph/9907348)

---

This preprint was prepared with the AAS L<sup>A</sup>T<sub>E</sub>X macros v4.0.

Table 2. Variable parameters for the stellar, dust and halo models

$\Sigma_{\text{extra}}$	$D_{\text{extra}}$	$W/w$	$\sigma$	$f_{\text{macho}}$
$0\text{-}50 M_{\odot} \text{pc}^{-2}$	40-60 kpc	0.5-2	20%-40%	0-0.5

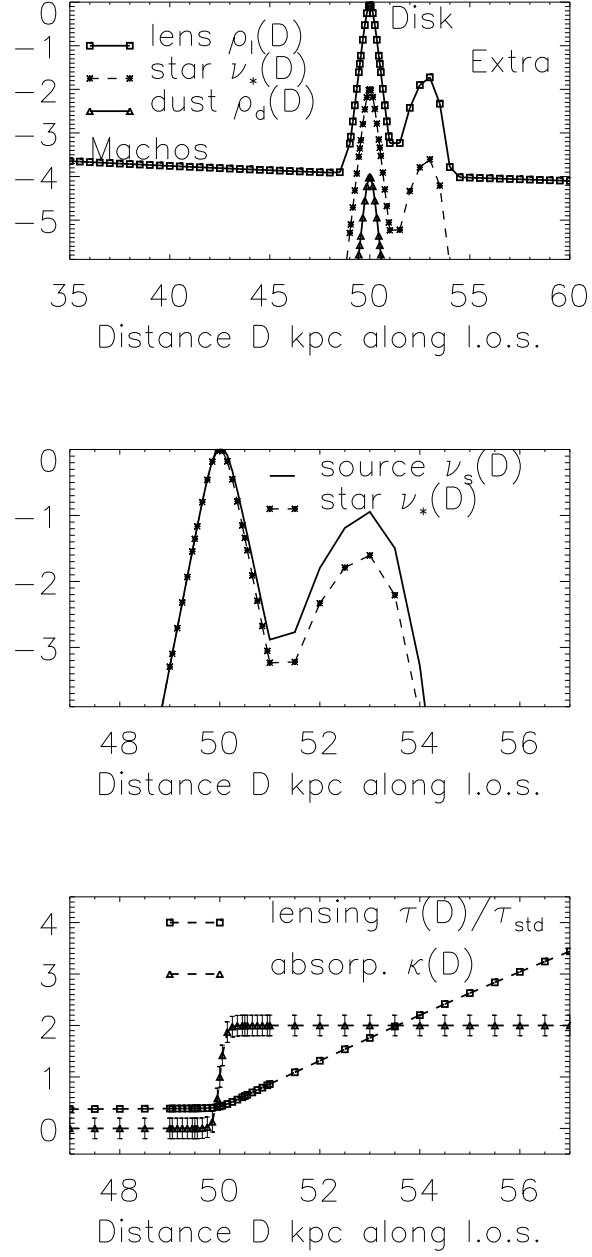


Fig. 1.— Upper panel: the density (in logarithmic scale with arbitrary zero point) of the lenses, the unlensed LMC stars and the density of the dust layer along the line of sight to the LMC. Middle panel: a zoom-in of the upper panel for the unlensed LMC stars and the lensed source stars. Lower panel: the run of the rescaled absorption of the dust (dashed lines with error bars) and the rescaled optical depth of microlensing (dashed line with squares) as functions of line of sight distance. The small error bars indicate a 20% dispersion due to patchiness and measurement error. All calculations are done for  $W = 2w = 400\text{pc}$ ,  $D_{\text{extra}} = 53\text{kpc}$ ,  $\Sigma_{\text{extra}} = 20M_\odot \text{pc}^{-2}$  and  $f_{\text{macho}} = 0.38$ .

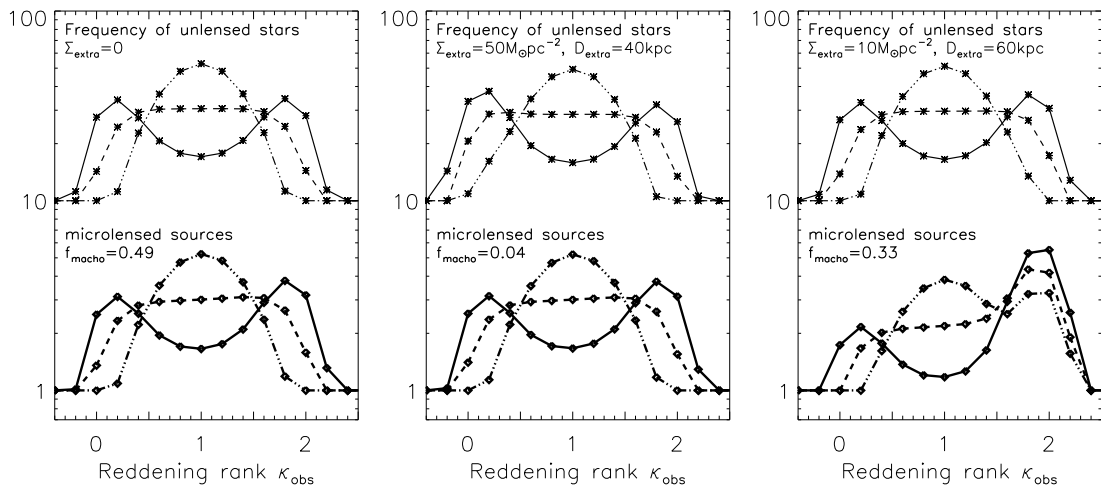


Fig. 2.— the frequency of finding stars with a certain rescaled reddening for the microlensed sources (the lower part of each panel) and the unlensed stars (the upper part of each panel). The legends show model parameters. Models are calculated for a thick disk and a thin dust layer with  $W = 2w = 400\text{pc}$  (solid lines), an equally thin disk and dust layer with  $W = w = 200\text{pc}$  (dashed lines), and a thin disk and a thick dust layer with  $W = w/2 = 100\text{pc}$  (dash-dot-dot lines). The distributions have been smoothed by a Gaussian with a dispersion  $\sigma = 20\%$  to allow for the measurement error and patchiness.

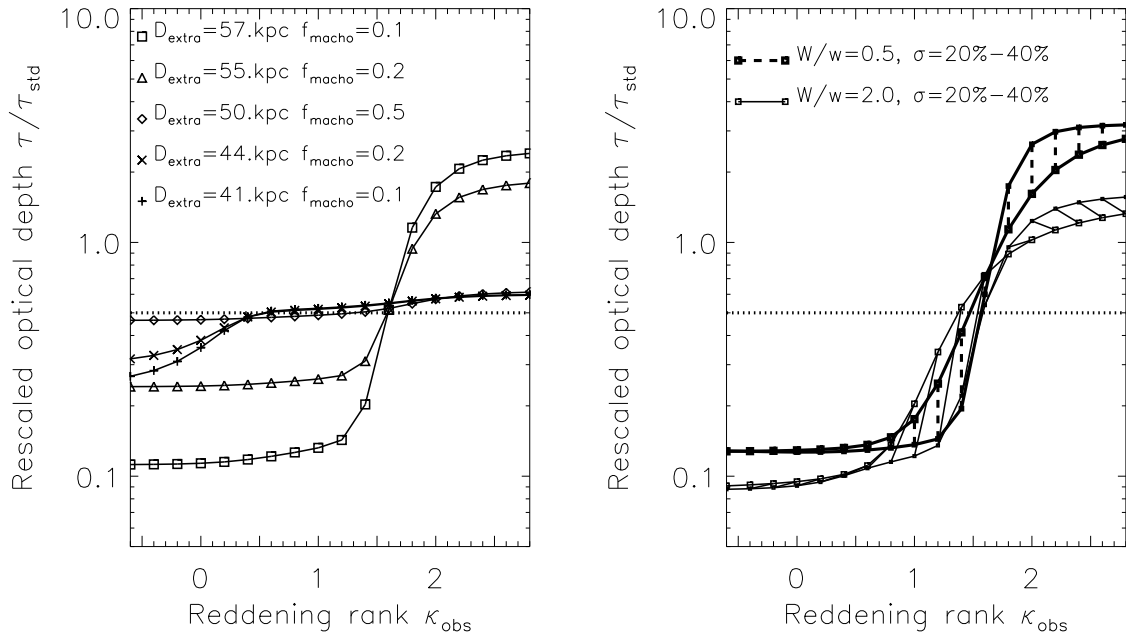


Fig. 3.— the optical depth, rescaled by that of the standard model  $\tau_{\text{std}}$ , as a function of the reddening for several models with  $\Sigma_{\text{extra}} = 50 M_{\odot} \text{ pc}^{-2}$ . Models are calculated for  $\sigma = 20\%$ ,  $W = w = 200 \text{ pc}$ , and a range of  $D_{\text{extra}} = 41 - 57 \text{ kpc}$  (left panel), and for  $D_{\text{extra}} = 57 \text{ kpc}$ , and a range of  $\sigma = 20\% - 40\%$  and  $W/w = 0.5 - 2$  (right panel). In the absence of stellar lenses, a halo model would predict the (horizontal dotted) line  $\tau_{\text{obs}}/\tau_{\text{std}} = 0.5$ .

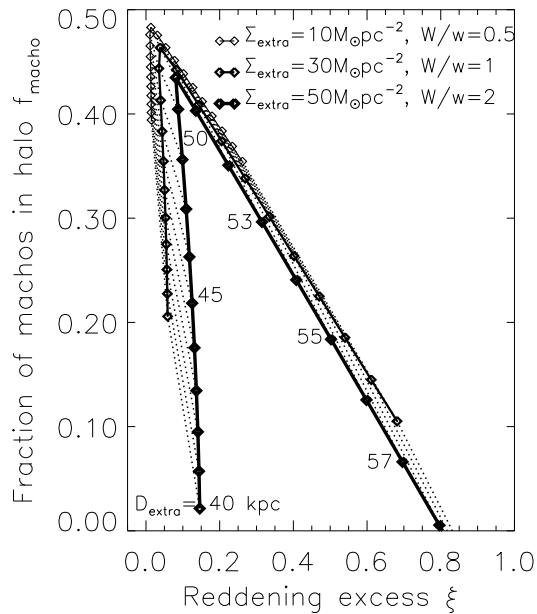


Fig. 4.— the excess reddening vs. the fraction of machos. We vary surface density  $\Sigma_{\text{extra}} = (10 - 50) M_{\odot} \text{ pc}^{-2}$  of the extra stars and its peak position  $D_{\text{extra}} = 40 - 60 \text{ kpc}$ . Each model allows a range of thickness for the dust layer  $w$  stellar disk and  $W$ . We trade between the amount of extra stars  $\Sigma_{\text{extra}}$  and the amount of machos  $f_{\text{macho}}$  such that models all have a fixed optical depth  $\langle \tau_{\text{obs}} \rangle / \tau_{\text{std}} = 0.5$ . The predictions are shown as three hatched bands.